

Supplementary figures

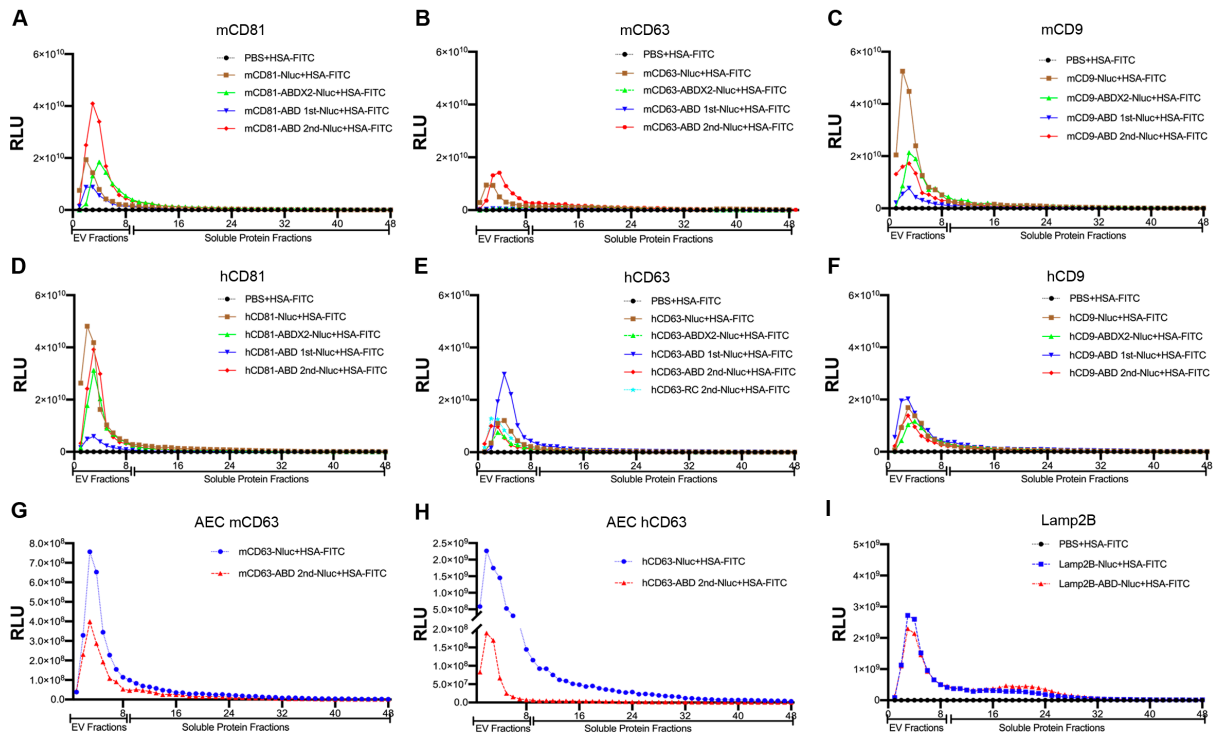


FIGURE S1. Nluc luciferase activities in different fractions after size exclusion. (A-F) Nluc luciferase activities in different fractions of tetraspanin-engineered ABD-EVs derived from HEK-293T cells after size exclusion (A: mCD81, B: mCD63, C: mCD9, D: hCD81, E: hCD63 and F: hCD9). (G) Nluc luciferase activities in different fractions of mCD63-engineered ABD-EVs derived from AEC cells after size exclusion. (H) Nluc luciferase activities in different fractions of hCD63-engineered ABD-EVs derived from AEC cells after size exclusion. (I) Nluc luciferase activities in different fractions of Lamp2B-engineered ABD-EVs derived from HEK-293T cells after size exclusion.

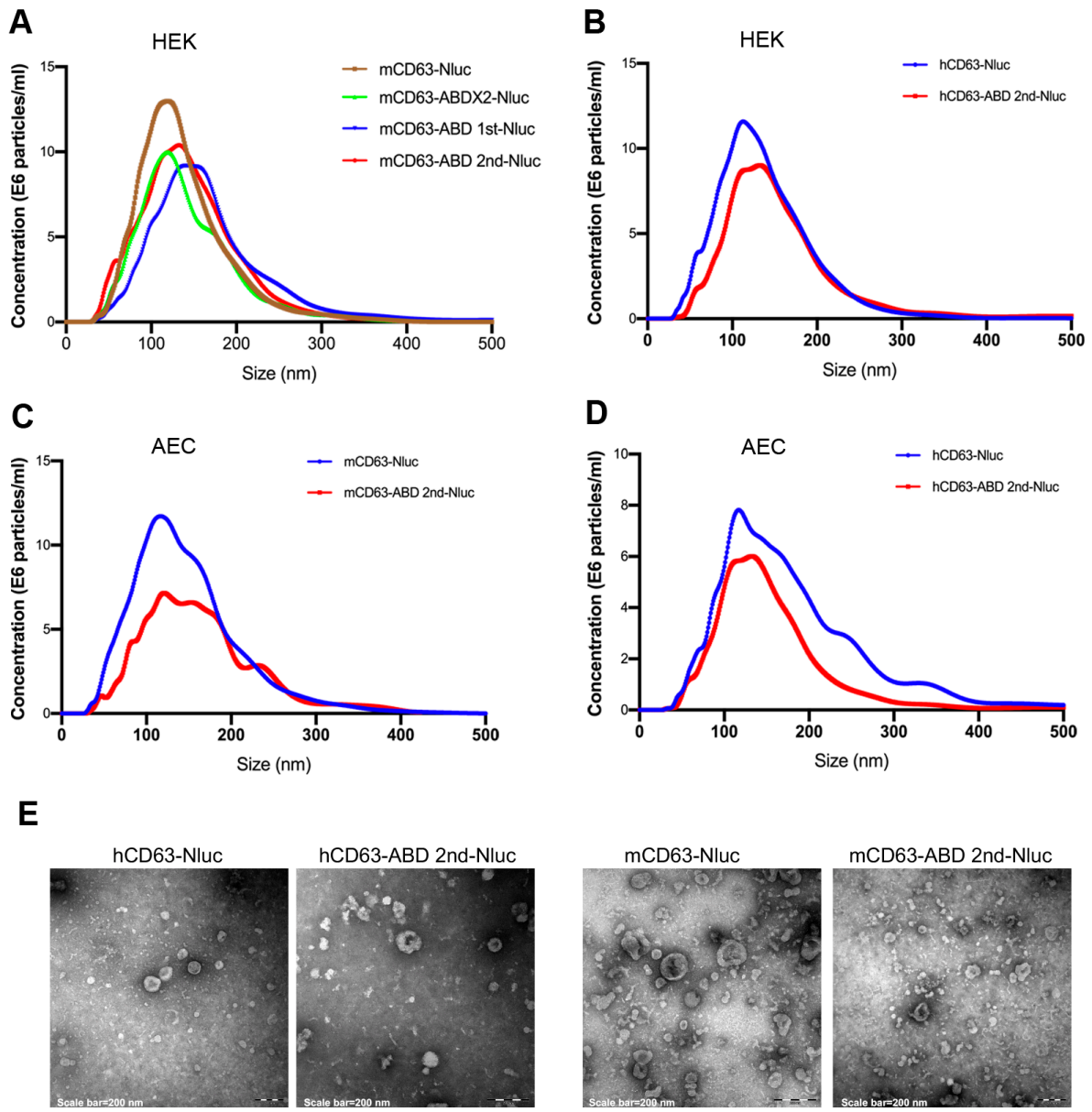
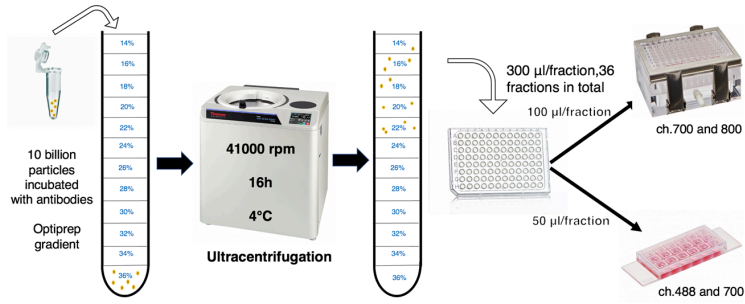
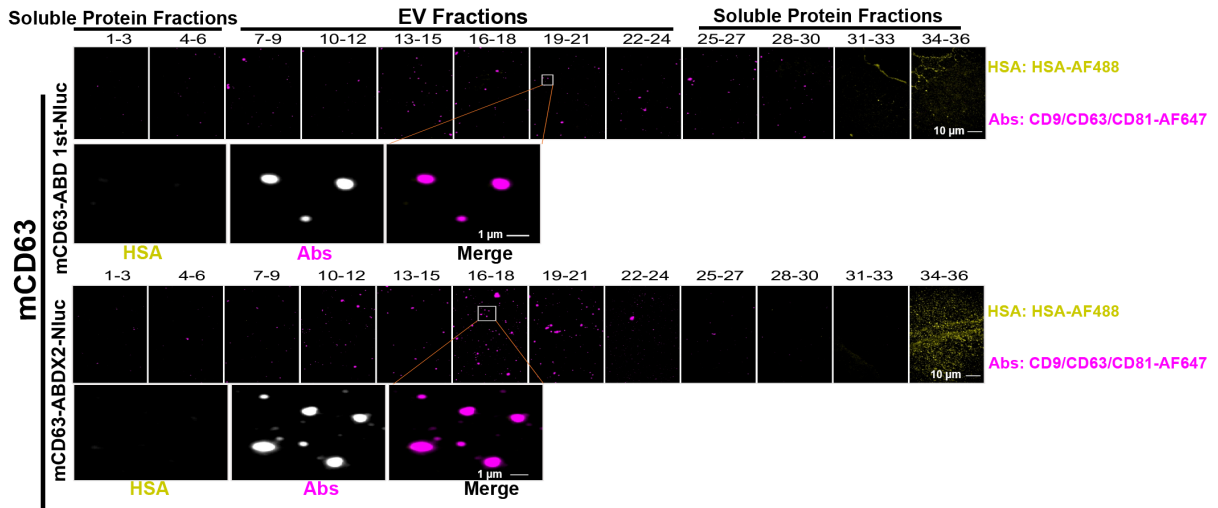


FIGURE S2. Characterization of the ABD-engineered EVs. (A-D) Size distributions of the ABD-engineered EVs measured by NTA. (E) The integrity and shape of ABD-engineered EVs bound by HSA evaluated by TEM.

A Procedure for Density Gradient Purification of EVs used for imaging



B



C

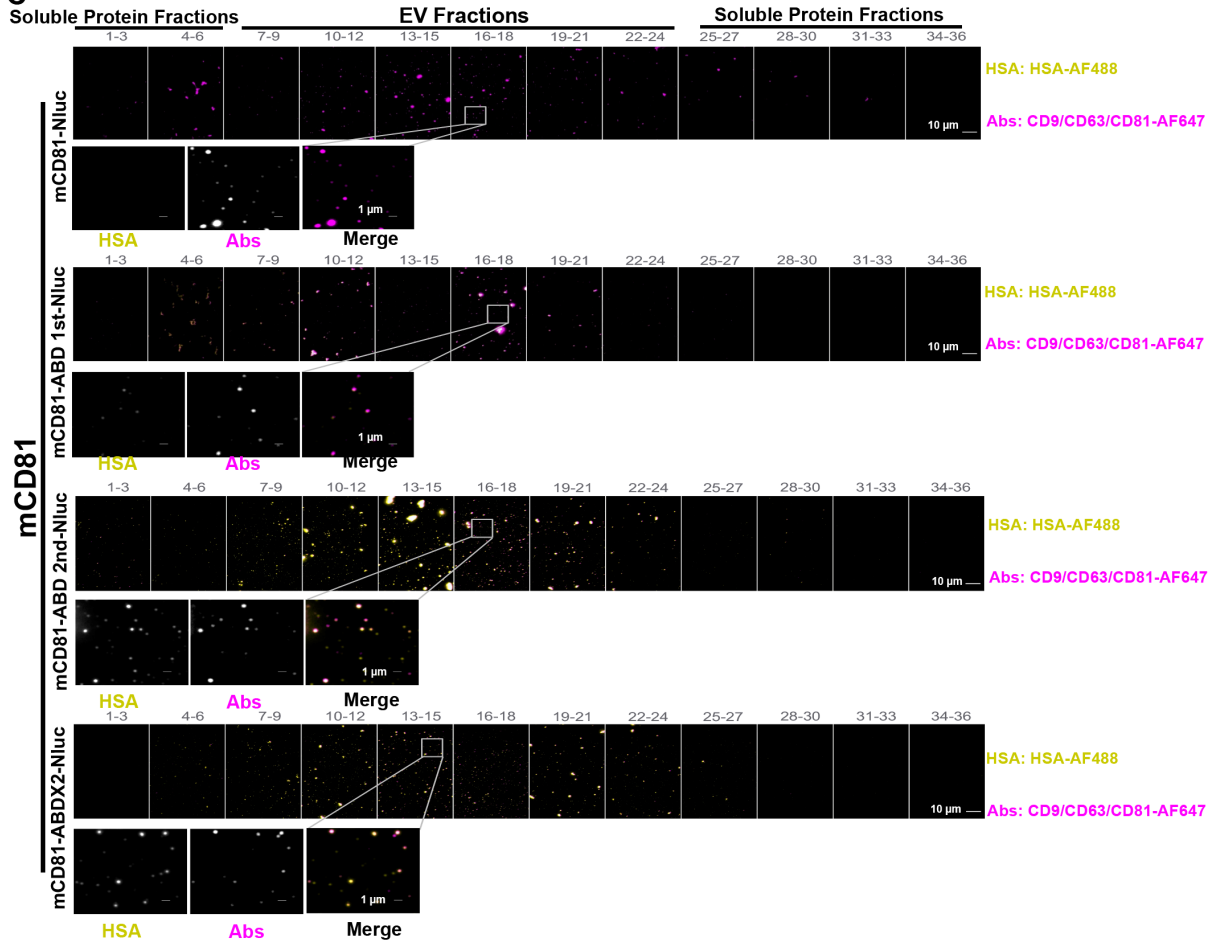
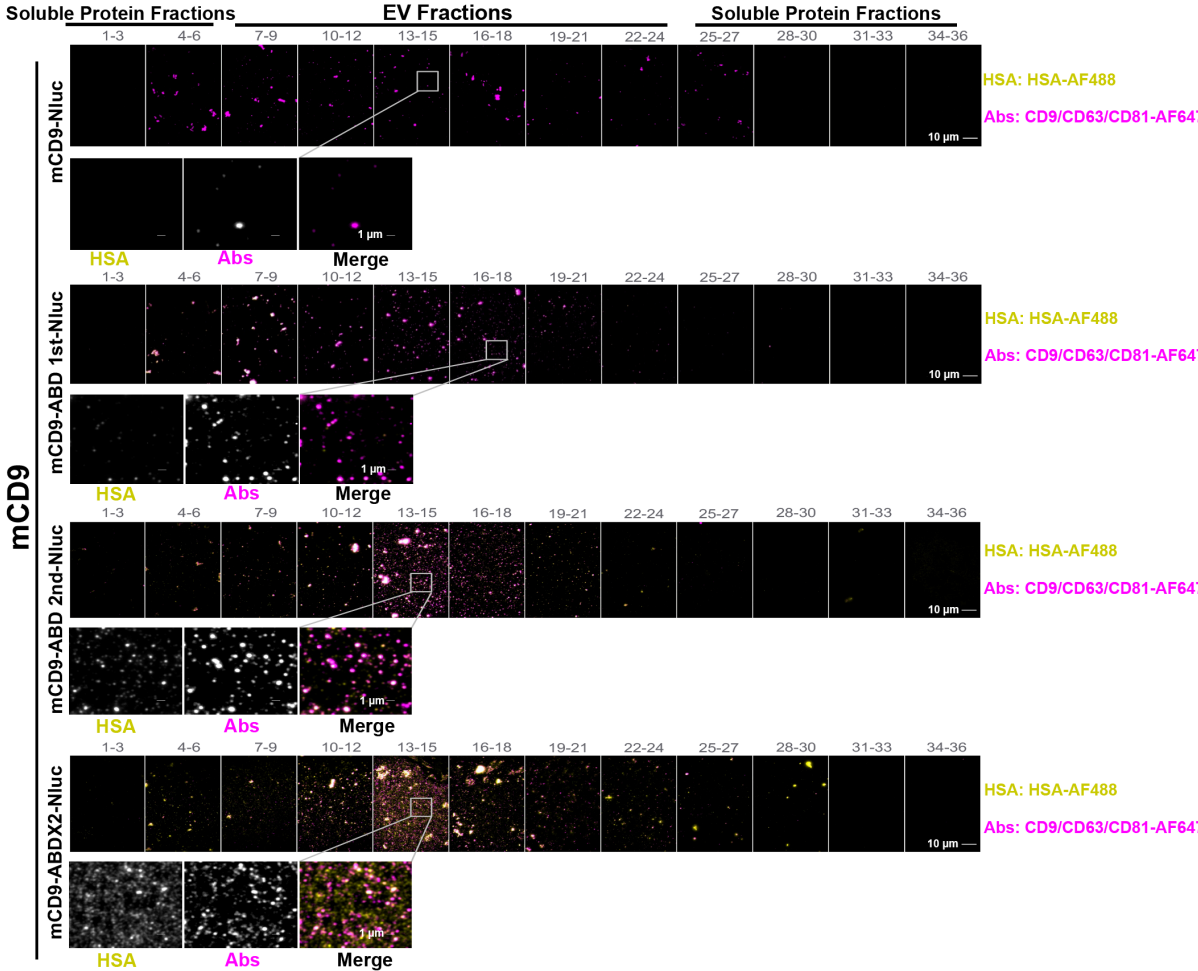


FIGURE S3. Procedure for density gradient purification of EVs for imaging and binding of tetraspanin-engineered EVs with HSA checked by imaging. (A) Schematic illustration of the workflow for density gradient purification of EVs for imaging. (B) Binding of mCD63-engineered EVs (ABD 1st and ABD×2) with HSA. (C) Binding of mCD81-engineered EVs with HSA.



FIGURES4. Binding of mCD9-engineered EVs with HSA checked by imaging.

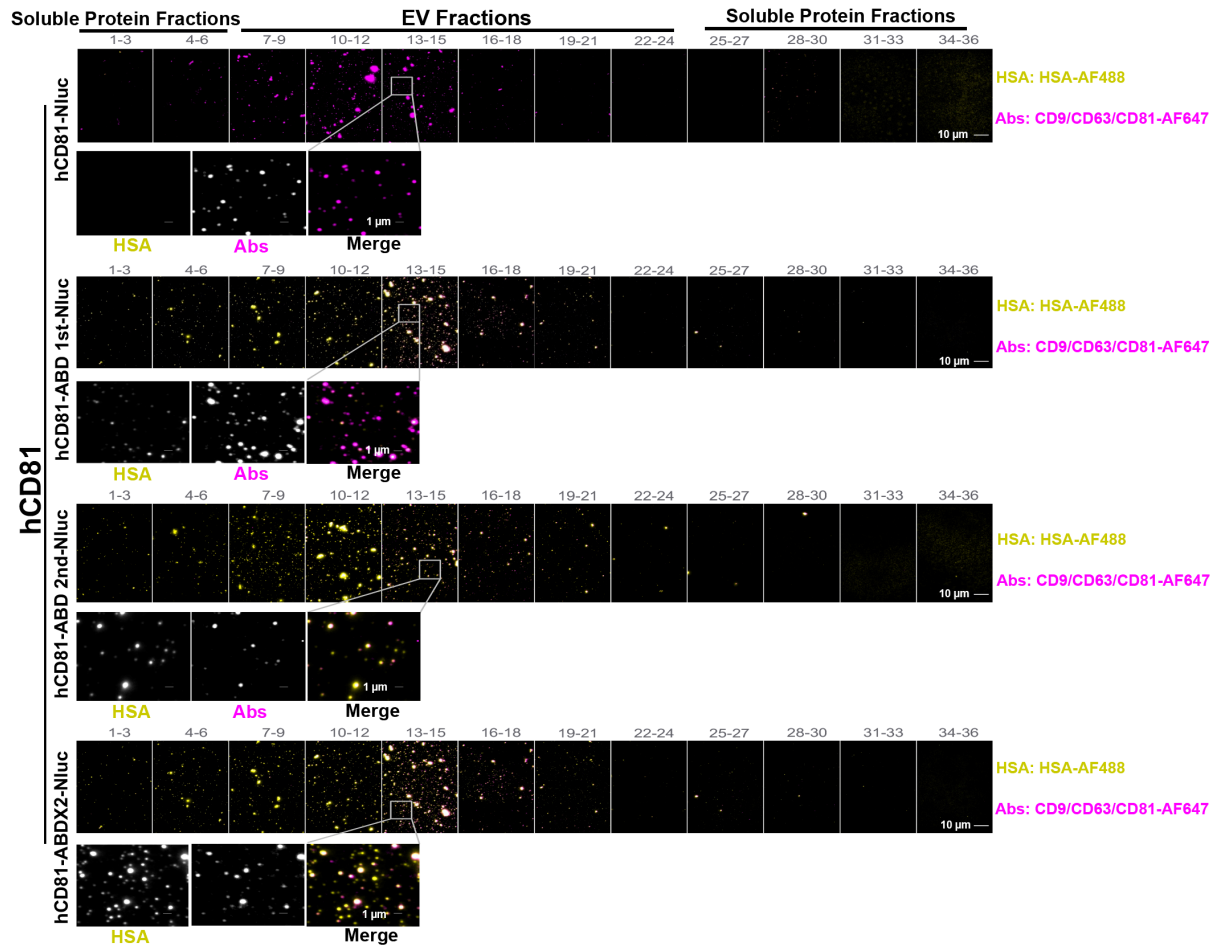


FIGURE S5. Binding of hCD81-engineered EVs with HSA checked by imaging.

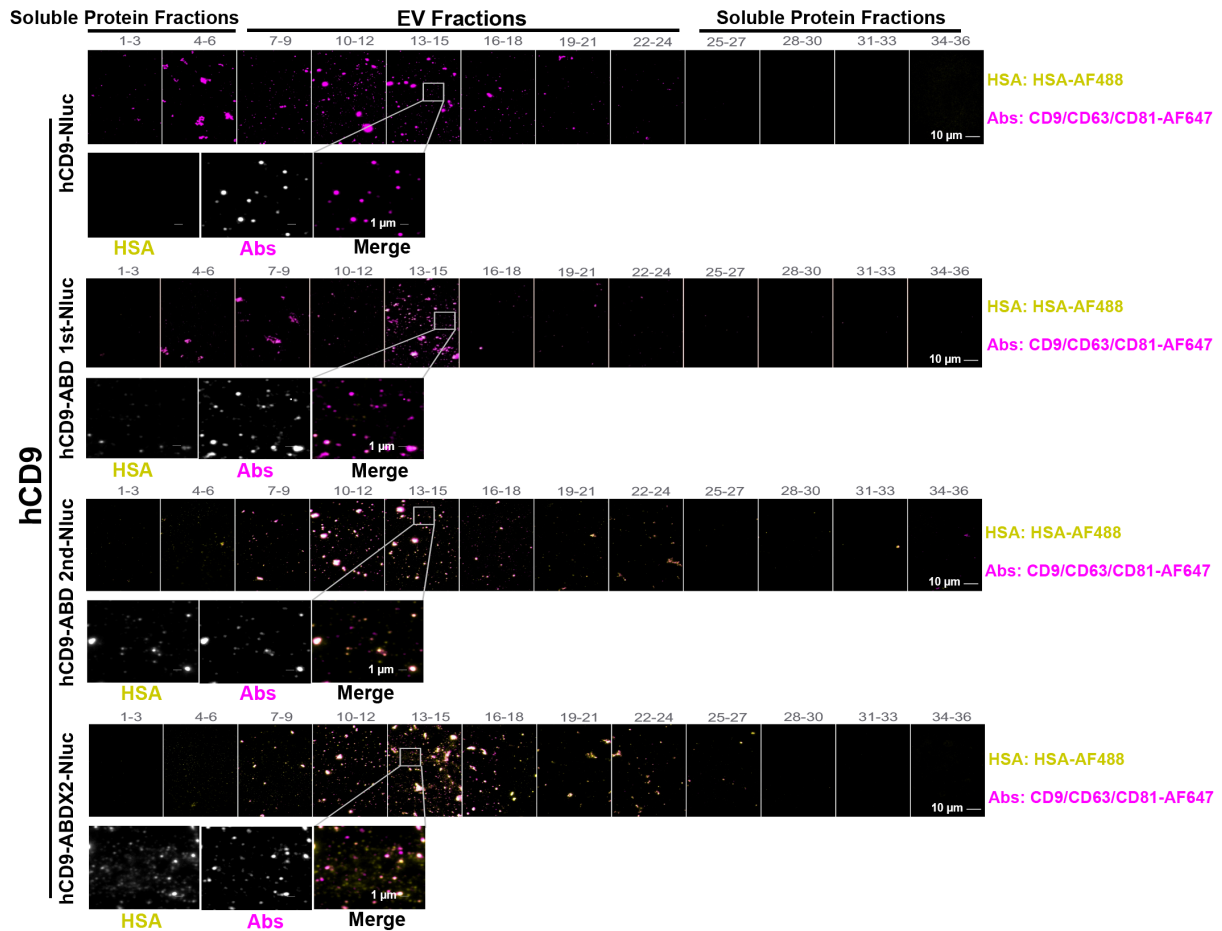


FIGURE S6. Binding of hCD9-engineered EVs with HSA checked by imaging.

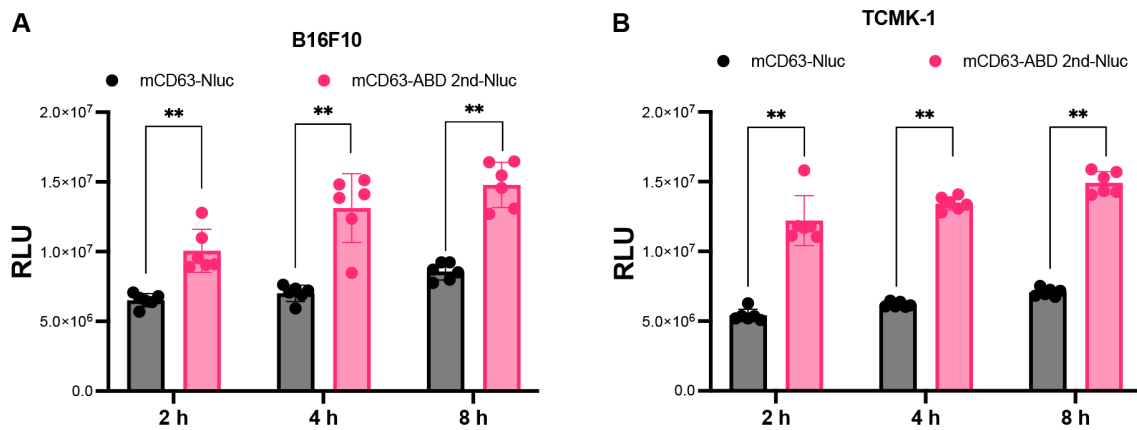


FIGURE S7. Uptake of ABD-EVs in B16F10 and TCMK-1 mouse cell lines. (A) Uptake of EVs at different time points in B16F10 cells. (B) EV-uptake at investigated time points in TCMK-1 cells.

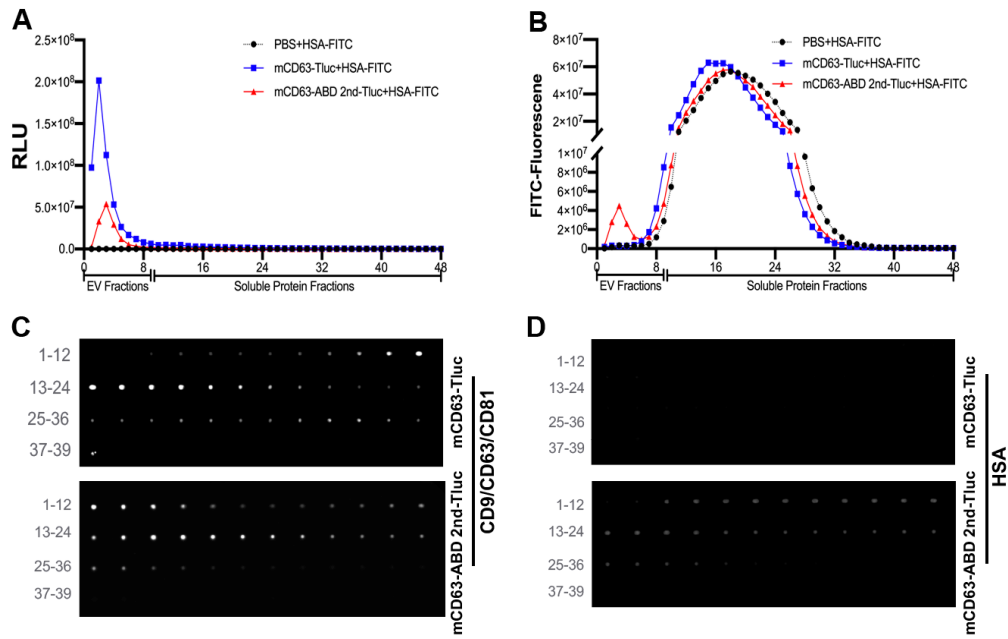


FIGURE S8. Luciferase activities and HSA binding of mCD63-ABD-Tluc EVs. (A) Tluc luciferase activities in different fractions of mCD63-engineered ABD-EVs derived from HEK-293T cells after size exclusion. (B) HSA binding of different fractions of mCD63-engineered ABD-EVs derived from HEK-293T cells after size exclusion. (C) HSA binding of different fractions of mCD63-engineered ABD-EVs derived from HEK-293T cells evaluated by widefield imaging.